

## On the low lying excited states of methyl amine

D. P. Taylor and E. R. Bernstein

Citation: *The Journal of Chemical Physics* **103**, 10453 (1995); doi: 10.1063/1.469895

View online: <http://dx.doi.org/10.1063/1.469895>

View Table of Contents: <http://aip.scitation.org/toc/jcp/103/24>

Published by the *American Institute of Physics*

---

---

**COMPLETELY**

**REDESIGNED!**



**PHYSICS  
TODAY**

*Physics Today* Buyer's Guide  
Search with a purpose.

# On the low lying excited states of methyl amine

D. P. Taylor and E. R. Bernstein

*Department of Chemistry, Colorado State University, Fort Collins, Colorado 80523*

(Received 12 July 1995; accepted 21 September 1995)

Mass resolved excitation spectroscopy (MRES) and high level *ab initio* calculations are employed to explore the low lying excited states of methyl amine,  $\text{CH}_3\text{NH}_2$ . Both (1+1) and (2+2) MRES of  $\text{CH}_3\text{NH}_2$  produce well resolved vibronic features in the energy region around 39 770 to 46 000  $\text{cm}^{-1}$ . A complete data set in this region for (2+2) MRES is presented for the isotopic series  $\text{CH}_3\text{NH}_2$ ,  $\text{CD}_3\text{NH}_2$ ,  $\text{CH}_3\text{ND}_2$ , and  $\text{CD}_3\text{ND}_2$ . Two apparent Franck–Condon progressions can be qualitatively characterized in these spectra. In order to identify the excited state vibrations active in these spectra and to identify the nature of the excited electronic state(s) accessed, a rather extensive set of *ab initio* calculations are undertaken. An open shell Hartree–Fock force constant calculation proves central to assigning the observed vibrations. Agreement between the predicted and observed vibrational frequencies provide the strongest evidence to date for a planar excited state C–NH<sub>2</sub> geometry. Using combinations and overtones of only two vibrations, the amine wag and scissors modes, all the major features of the low energy region of the spectra can be assigned for all the isotopically substituted methyl amines. *Ab initio* calculations indicate that the lowest *A'* excited state is an *A'* 3*s* Rydberg and the lowest *A''* excited state is a valence electronic state. An additional *A'* 3*s* Rydberg state is also found in this region, which because of its geometry, can be implicated in the methyl hydrogen elimination photodissociation reaction of methyl amine. Complete active space self-consistent field (CASSCF) calculations alone, and augmented by many body perturbation theory (MBPT), are also performed. The spectra are consistent with two excited electronic states in the 40 000  $\text{cm}^{-1}$  region. This new characterization of the low energy absorption spectra, and the interpretation of the high energy region in terms of an addition electronic state, challenge the long held view of the nature of the methyl amine excited states. © 1995 American Institute of Physics.

## I. INTRODUCTION

The lowest excited states of simple alkyl amines are typically thought to be of a 3*s* nitrogen Rydberg atomic character.<sup>1,2</sup> This description arises from a nitrogen lone pair 2*p* electron promotion to a localized nitrogen atomic 3*s* orbital. Based on a study of azabicyclooctanes ( $\text{C}_6\text{N}_2\text{H}_{12}$ , DABCO, and  $\text{C}_7\text{NH}_{13}$  ABCO) we have concluded that this picture of a low-lying Rydberg state of an amine as an excitation which is localized on the nitrogen atom in general, and the nitrogen 3*s* orbital in particular, is not very useful.<sup>3,4</sup> With this report, we expand our studies of the low-lying excited electronic states of alkyl amines to include methyl amine. The excited states of ammonia have received considerable attention in the past,<sup>5–7</sup> but alkyl substituted ammonias have not been the subject of such experimental or theoretical scrutiny.

Methyl amine is a small, low symmetry molecule with at least two degrees of large amplitude internal motion: methyl rotation and “amine” inversion at the nitrogen atom. Additionally, methyl amine has a large geometry change upon electronic excitation. Previous spectroscopic studies of methyl amine are plagued by intense hot band structure, broad features, and long Franck–Condon progressions. Methyl amine readily forms dimers and higher multimers; these species contribute to nonmass detected spectra of methyl amine and thereby can confuse and complicate the data set even further. Ground state methyl amine has been studied by infrared,<sup>8–11</sup> microwave,<sup>12,13</sup> and other spectroscopic techniques.<sup>14–16</sup> In the ground state, methyl amine has ap-

proximately the structure of ethane with the lone pair on the nitrogen occupying the position of one of the ethane hydrogen atoms. Methyl amine has an “inversion mode” much like that characterized for ammonia. This inversion mode couples to the large amplitude methyl rotor motion and other vibrations and leads to rather complicated dynamics in the ground state. These motions have recently been treated by Hougen and collaborators.<sup>17–21</sup>

The uv absorption spectrum of methyl amine has been studied by a number of groups, dating back to the 1930s. Herzberg and Kolsch<sup>1</sup> explained the similarity between the spectrum of ammonia and simple amines (including methyl amine) by proposing that the first excited state of these species is a 3*s* Rydberg state localized on the nitrogen atom. Förster and Jurgens<sup>22</sup> analyzed their methyl amine spectra in terms of two vibrational frequencies; this approach has been followed in most of the subsequent studies.

The effort to analyze the methyl amine electronic absorption spectrum in the near ultraviolet has focused on identification of the assumed two active vibrational modes and the location of the origin of the transition. Förster and Jurgens<sup>22</sup> report 41 680  $\text{cm}^{-1}$  as the origin of this absorption while Tannenbaum *et al.*<sup>23</sup> suggest the origin at 41 690  $\text{cm}^{-1}$ . More recently, Tusboi *et al.*<sup>24,25</sup> report the origin at 41 715  $\text{cm}^{-1}$ . None of these studies rely on mass resolution for the detection scheme nor are their samples cooled sufficiently to eliminate hot band structure in the spectra.

Mulliken<sup>2</sup> used Herzberg’s suggestion that the first excited state of methyl amine consists of a half-filled 3*s* Rydberg orbital and a half-filled nonbonding 2*p* orbital isolated

on the nitrogen atom in his discussion of trends in the ammonia–amine series. Perhaps more than any other contribution to the methyl amine literature, Mulliken's paper has had a profound influence on later work. The expectation that the first excited state of methyl amine would have a geometry in which carbon, nitrogen, and amine hydrogens all lie in a single plane is also tied to these early discussions. For the past 60 years, the prediction that the first excited state of methyl amine (at ca.  $40\,000\text{ cm}^{-1}$ ) is a  $3s$  Rydberg state largely isolated on the nitrogen atom has seemed to be the only viable explanation for its electronic spectroscopy.

The geometry and electronic structure of methyl amine in its first excited electronic state are far less well established than are those of the ground state. Since Förster and Jurgens<sup>22</sup> in 1937, several studies of the ultraviolet absorption spectra of methyl amine have concluded that two vibrational frequencies ( $650$  and  $1000\text{ cm}^{-1}$ ) can be used to explain the broad, nearly periodic structure observed in the  $40\,000$  to  $45\,000\text{ cm}^{-1}$  energy region. The assignment of these two frequencies as amine-wagging and methyl rocking is suggested by Tsuboi *et al.*<sup>24,25</sup> to support the claim of a ( $\text{C}-\text{NH}_2$ ) planar excited state, but the data upon which this claim is based are not very convincing. In general, the prior studies of methyl amine electronic structure have had insufficient experimental resolution or have lacked the calculational sophistication required to inspire confidence in the assignment of excited state methyl amine origin, vibrations or geometry.

The trends within the ammonia–amine series are as interesting today as they were 60 years ago when first addressed by Herzberg and Mulliken. The excited state electronic and vibrational structure of these molecules are tractable calculations at a rather high level of *ab initio* theory.<sup>26,27</sup> The excited states of ammonia are comparatively well understood both theoretically and experimentally. The experimental study of excited state hydrazine ( $\text{H}_2\text{N}-\text{NH}_2$ ) has proven to be a very difficult problem and progress has been slow despite the interest in hydrazine<sup>28</sup> as an “energetic material.” The properties of methyl amine fall between those of ammonia and hydrazine and, as such, might offer some theoretical and experimental insights into these other systems.

In this report, we present new experimental and calculational results for methyl amine and its deuterated isotopic analogs. Our contributions for an improved experimental data set arise due to extreme supersonic cooling; methyl amine spectra in the past have been plagued by complex and unanticipated contributions from excited ground state motions. Our contribution for an improved calculational data set include vibrational frequencies for ground and excited states and rather extensive inclusion of configuration interaction for ground and excited state wave functions within the context of a number of different approaches.

## II. PROCEDURES

### A. Experiment

The  $\text{CH}_3\text{NH}_2$  sample is used directly from the lecture bottle and mixed with carrier gas for expansion through a

supersonic nozzle into the vacuum chamber. All methyl amine used in this study is purchased from Aldrich, Inc. The isotopic samples are obtained as  $\text{CD}_3\text{NH}_2\cdot\text{HCl}$ ,  $\text{CH}_3\text{ND}_2\cdot\text{DCl}$ , and  $\text{CD}_3\text{ND}_2\cdot\text{DCl}$ . The  $\text{CD}_3\text{NH}_2\cdot\text{HCl}$  sample is placed in an evacuated glass vessel with a frozen sodium hydroxide aqueous solution and heated.<sup>24</sup> Since it is difficult to drive the methyl amine from the solution, the procedure works best if the solution volume is kept to a minimum. The  $\text{CD}_3\text{NH}_2$  produced in this manner is collected in a cold trap cooled with liquid nitrogen.  $\text{CH}_3\text{ND}_2\cdot\text{DCl}$  and  $\text{CD}_3\text{ND}_2\cdot\text{DCl}$  are processed in like manner with  $\text{NaOD}$  and  $\text{D}_2\text{O}$  solutions.

Methyl amine is introduced into a time-of-flight mass spectrometer vacuum system through a pulsed nozzle with  $20\text{ psi}$  ( $\sim 200\text{ kPa}$ ) backing pressure. The general apparatus for these studies is given in the literature.<sup>29</sup> Early in this series of experiments, the gas sample contained approximately 1% methyl amine, 4%  $\text{CF}_4$ , and 2% propane in helium. The (1+1)-mass resolved excitation-ionization spectra (MRES) of  $\text{CH}_3\text{NH}_2$  are obtained with this mixture. All of the later (2+2) spectra are, however, obtained with an expansion mixture of 2% methyl amine in neon 70 (70% Ne and 30% He).

The (1+1) MRES experiment is performed using doubled dye laser output mixed with  $1064\text{ nm}$  light from a Nd/YAG/dye laser pump system. The doubled and mixed light is separated from the dye laser fundamental, doubled dye output, etc., using either a Pellin-Broca prism or a broadband  $240\text{ nm}$  dichroic beam splitter. The beam energy per pulse is roughly  $0.5\text{ mJ}$ . The laser beam is loosely focused by either a  $35$  or  $50\text{ cm}$  lens on the molecular beam in order to obtain increased signal-to-noise ratio for the final data collection.

The (2+2) MRES are obtained using the same Nd/YAG/dye laser combination with several coumarin dyes (C440, C460, C480) pumped at  $355\text{ nm}$  (tripled Nd/YAG fundamental). The dye laser energy in this configuration is typically  $15\text{ mJ/pulse}$ . Again a  $35$  or  $50\text{ cm}$  lens is employed to focus the blue light on the molecular beam; in this case, however, the light is tightly focused in the molecular beam. The (2+2) resonant enhanced multiphoton ionization process is detected by a microchannel plate detector.

### B. Theory

All reported *ab initio* calculations are performed with the HONDO 8.5 suite of programs<sup>30</sup> running on an IBM RS 6000 RISC workstation. The basis set for all calculations reported is double zeta valence plus polarization functions (dzp), augmented as appropriate with  $3s$  functions on nitrogen and carbon to allow for Rydberg state excitation. These additional functions have little or no effect on ground state methyl amine properties. Initial calculations with  $3s$  and  $3p$  basis set augmentation were tested but since no  $3p$  functions appeared in the ground or relevant excited state wave functions, they were dropped from the basis set.

Both open and closed shell restricted Hartree–Fock (RHF) calculations are performed with geometry optimization. Open shell RHF calculations are carried out for the  $A'$  ground state and for the lowest energy excited states of  $A'$  and  $A''$  symmetry.

The above RHF calculations are used as initial structure and wave function guesses for the multiconfiguration single and double excitation (MCSD) calculation subsequently performed. All but two core orbitals are allowed in the excitations (singles and doubles); a  $1s$  carbon and a  $1s$  nitrogen orbital are frozen in the core. All 29 orbitals from the dzp RHF level are used in the  $A'$  MCSD calculations: for the  $A''$  excited states only 28 orbitals could be included in the initial guess due to HONDO limitations. All MCSD calculations include geometry optimization.

HONDO 8.5 also supports complete active space (CAS) and CAS with many body perturbation theory (CASS-CFMBPT) calculations. Both of these methods explore effects of configuration interaction on structure, excitation, and electronic distribution, but each in a manner different from the other two (as will be demonstrated below). The opportunity to compare several approaches to excited state *ab initio* calculations and experimental results for a low symmetry polyatomic molecule is exploited here.

### III. RESULTS

#### A. Experiment

We have gone to considerable effort to cool methyl amine by varying the pulsed valve supersonic expansion conditions and the carrier gas. Although cooling remains a problem, much of the present success with the analysis of the methyl amine spectra is due to the improved resolution achieved with reduction of hot band intensity. None of the vibronic features presented in the figures are assigned as a hot band transition and resolved feature widths seem to be controlled by residual internal rotational structure based on D/H isotopic substitution. Additionally, mass detected spectroscopy aids in the data analysis because methyl amine clusters very efficiently in the extreme cooling expansion conditions. Absorption associated with methyl amine clusters and photofragmentation is thereby avoided.

The (1+1)-MRES of methyl amine is presented in Fig. 1. Only the lowest energy region of the spectrum is shown. The structure associated with the first feature at  $41\,684\text{ cm}^{-1}$  is consistent with that expected for a hindered methyl rotor. The separation between the first two features in this group is  $30\text{ cm}^{-1}$ . Similar structure is observed (see below) for  $\text{CD}_3\text{ND}_2$  but with one-half the spacing. The full width at half height for the most intense feature displayed is  $\sim 15\text{ cm}^{-1}$ .

In the (1+1)-MRES experiment, mass peaks are observed that are consistent with dimer, trimer, and still larger clusters of methyl amine. The monomer mass channel is found in a series of mass peaks that are separated by 1 amu. The nozzle-laser timing delay is critical in the acquisition of the (1+1)-MRES because the relatively small methyl amine signal must be maximized with respect to the much larger feature that appears at one higher mass unit. The signal in the latter mass channel is most likely due to photofragmentation of the methyl amine dimer.

Because of its low symmetry, selection rules for one- and two-photon spectroscopy of methyl amine are essentially the same in linearly polarized light at vibrational resolution. The (2+2)-MRES experiment turns out to be easier to ac-

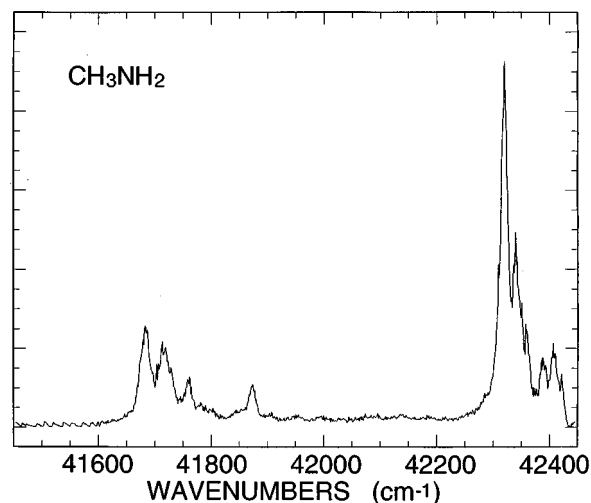


FIG. 1. (1+1) Mass resolved excitation spectrum (MRES) of methyl amine. The lowest energy features of the spectrum exhibit hindered methyl rotor structure. The largest peak has a full width at half maximum of  $15\text{ cm}^{-1}$ .

quire in that interference from higher multimers and background signals appear to be reduced, and the ion signal in the methyl amine mass channel is larger. The (2+2)-MRES of methyl amine is presented in Fig. 2. The features in the (2+2) spectra are slightly broader than those in the (1+1) spectra; this may be due to either power broadening or a variation in the expansion conditions. The carrier gas for all the (2+2)-MRES is neon 70, which shows a marked improvement in signal/noise ratio and better reproducibility in the expansion conditions. Reduction in the mass peak at 1 amu higher mass than methyl amine eliminates much of the unwanted background signal and allows the methyl amine mass channel features to be the most intense in this group of mass channels. The (2+2)  $\text{CH}_3\text{NH}_2$  spectrum of Fig. 2 covers three laser dye ranges. The lower energy region exhibits sharp, relatively well-resolved peaks while the high energy region of this spectrum consists of broader peaks of regularly decreasing intensity. The spacing between these latter features is roughly  $325\text{ cm}^{-1}$ .

The (2+2)-MRES of several deuterated methyl amines are presented in Figs. 3, 4, and 5. The excitation spectroscopic data for all the methyl amine isotopes studied ( $\text{CH}_3\text{NH}_2$ ,  $\text{CH}_3\text{ND}_2$ ,  $\text{CD}_3\text{NH}_2$ , and  $\text{CD}_3\text{ND}_2$ ) are tabulated in Tables I through IV.

#### B. Theory

##### 1. RHF

The energy and geometry for the ground state and lowest energy  $A'$  and  $A''$  states of methyl amine based on an RHF dzp basis set calculation are presented in Table V. The closed shell ground state is, of course, of  $A'$  ( $C_s$ ) symmetry. The geometry is similar to that of ethane, with the lone pair electrons on the nitrogen atom taking the place of one of the ethane hydrogen atoms.

The open shell RHF dzp basis set, augmented with  $3s$  orbitals (dzp+3s) generates a lowest excited state of  $A'$  symmetry. As expected from the literature, this state can be characterized as a  $3s$  Rydberg state and its geometry is found

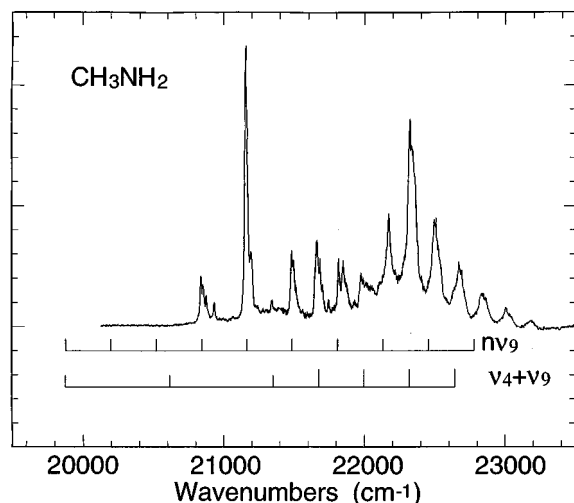


FIG. 2. (2+2) MRES of  $\text{CH}_3\text{NH}_2$ . The lines below the spectrum indicate the  $\nu_9$  amine wagging vibration. Below the lines for the  $\nu_9$  progression, a progression in  $\nu_9$  built upon two quanta of  $\nu_4$  (the amine scissors mode) is indicated. Combinations of these two vibrations are adequate to explain all the significant peaks in the low energy region (below  $22\,000\text{ cm}^{-1}$ ) of the spectrum.

to be such that the C-NH<sub>2</sub> moiety of the molecule is planar. An examination of the excited open shell orbital wave function reveals that the lowest  $3s$  Rydberg state has a large contribution from both the nitrogen  $3s$  atomic orbital (unnormalized occupation number 1.41) and the carbon  $3s$  atomic orbital ( $-0.39$ ). The next state higher in energy is also a  $3s$  Rydberg state (both  $3s$  nitrogen and carbon atomic orbitals contribute) and the lowest state of  $A''$  symmetry is a valence (no  $3s$  contribution) state. The second  $3s$  Rydberg state function has a larger contribution from the carbon  $3s$  orbital than from the nitrogen  $3s$  orbital. This second Rydberg state moves toward a "distorted" molecular geometry with two methyl hydrogens displaced so that the carbon atom can have an  $sp^2$ -like bonding structure. This distortion may suggest a role for the low lying  $3s$  Rydberg state in the photodissocia-

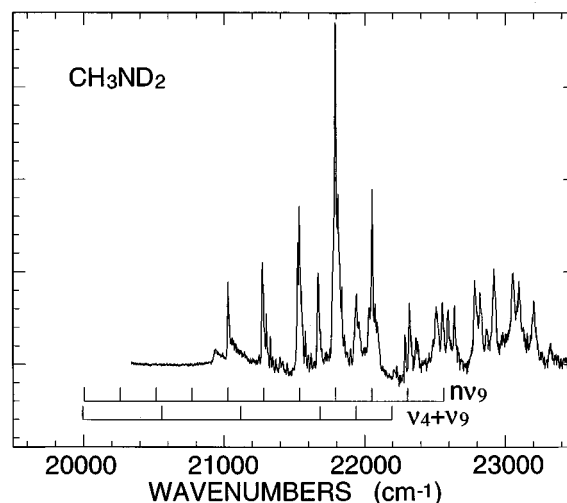


FIG. 4. (2+2) MRES of  $\text{CH}_3\text{ND}_2$ . See caption to Fig. 2 for more information. A progression in  $\nu_4 + \nu_9$  is indicated in addition to the  $n\nu_9$  progression.

tion chemistry of methyl amines. A recent publication suggests that  $\text{CH}_3\text{NH}_2$  photodissociates to  $\text{CH}_2\text{NH}_2$  if excited to the higher energy end of the spectral region shown in Figs. 2 through 5.<sup>31</sup>

Force constant calculations are also performed at the RHF level for the first three electronic states of methyl amine using a first derivative two-point difference method. The vibrational energies and descriptions for the first  $A'$  and  $A''$  excited states are found to be quite similar. The RHF vibrational energy results are scaled by the factor 0.9, as is usual to correct for an expected overestimation in HF vibrational predictions. Calculated vibrational energies for the  $3s$  Rydberg state  $A'$  are summarized in Table VI. An attempt is made to name these vibrations following the ground state numbering of Lord and Grey.<sup>8</sup> The low energy methyl torsional vibration has not been included in the list of Table VI. The motions associated with the calculated vibrational modes are indicated in Fig. 6 for various projections.

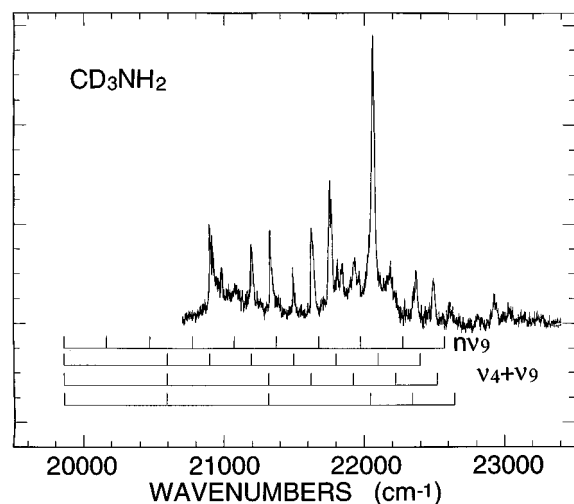


FIG. 3. (2+2) MRES of  $\text{CD}_3\text{NH}_2$ . See caption to Fig. 2 for more information. Three progressions in  $\nu_4 + \nu_9$  are indicated in addition to the  $n\nu_9$  progression.

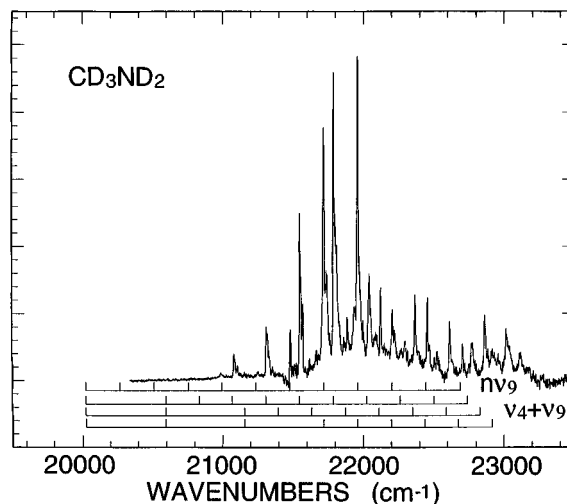


FIG. 5. (2+2) MRES of  $\text{CD}_3\text{ND}_2$ . See caption to Fig. 2 for more information. Three progressions in  $\nu_4 + \nu_9$  are indicated in addition to the  $n\nu_9$  progression.

TABLE I. CH<sub>3</sub>NH<sub>2</sub> spectrum. Assignments based on a transition origin of 39 770 cm<sup>-1</sup>.

Transition energy (cm <sup>-1</sup> )	Assignment	Tentative assignment
41 690	3ν <sub>9</sub>	
41 703		Hindered rotor feature
41 750		Hindered rotor feature
41 861		Hindered rotor feature
42 334	4ν <sub>9</sub>	
42 704	2ν <sub>4</sub>	
42 974	5ν <sub>9</sub>	1ν <sub>13</sub> +2ν <sub>14</sub>
43 340	1ν <sub>9</sub> +2ν <sub>4</sub>	
43 650	6ν <sub>9</sub>	
43 712	4ν <sub>9</sub> +1ν <sub>6</sub>	
43 768	4ν <sub>9</sub> +1ν <sub>12</sub>	
43 996	2ν <sub>9</sub> +2ν <sub>4</sub>	
44 062		3ν <sub>5</sub> ; 2ν <sub>14</sub> +3ν <sub>9</sub>
44 240		7ν <sub>9</sub>
44 357		5ν <sub>9</sub> +1ν <sub>6</sub>
44 649	3ν <sub>9</sub> +2ν <sub>4</sub>	
45 024		3ν <sub>4</sub> +1ν <sub>13</sub> ; 1ν <sub>1</sub> +2ν <sub>14</sub>
45 359		6ν <sub>8</sub> ; 2ν <sub>14</sub> +5ν <sub>9</sub> ; 1ν <sub>4</sub> +3ν <sub>6</sub>
45 683		7ν <sub>9</sub> +1ν <sub>12</sub>
46 007		6ν <sub>9</sub> +2ν <sub>14</sub>
46 371		6ν <sub>9</sub> +2ν <sub>6</sub>

## 2. MCSD

Using the RHF results as a starting point, a multiconfiguration self-consistent field calculation with single and double configuration interaction excitations (MCSD) is carried out. The advantage of this approach is that all virtual orbitals can be included in the calculation; however, the inclusion is only for single and double excitations from the reference configuration. Methyl amine is a low symmetry molecule and the energy separation between orbitals is not very large, so selection of virtual orbitals to include in the CI is not simple. Since methyl amine is a small molecule, a calculation is possible that freezes only two filled orbitals: a 1s nitrogen and a 1s carbon orbital.

The ground state MCSD calculation is carried out with a geometry search for a dzp basis set. The ground state geometry obtained in this manner is similar to that obtained by Davidson for a higher level calculation.<sup>26</sup> The calculation

TABLE II. CD<sub>3</sub>NH<sub>2</sub> spectrum. Assignments based on a transition origin of 39 703 cm<sup>-1</sup>.

Transition energy (cm <sup>-1</sup> )	Assignment	Tentative assignment
41 781	1ν <sub>9</sub> +1ν <sub>4</sub>	
42 380	2ν <sub>9</sub> +1ν <sub>4</sub>	
42 649		2ν <sub>4</sub> ; 5ν <sub>9</sub> ; 3ν <sub>12</sub>
42 969	3ν <sub>9</sub> +1ν <sub>4</sub>	
43 244	1ν <sub>9</sub> +2ν <sub>4</sub>	
43 493		4ν <sub>9</sub> +1ν <sub>4</sub>
44 118		5ν <sub>9</sub> +1ν <sub>4</sub>
44 736	1ν <sub>9</sub> +3ν <sub>4</sub>	
44 987		9ν <sub>9</sub> ; 4ν <sub>9</sub> +2ν <sub>4</sub>
45 843		3ν <sub>9</sub> +3ν <sub>4</sub> ; 5ν <sub>9</sub> +3ν <sub>5</sub>

TABLE III. CH<sub>3</sub>ND<sub>2</sub> spectrum. Assignments based on a transition origin of 39 985 cm<sup>-1</sup>.

Transition energy (cm <sup>-1</sup> )	Assignment	Tentative assignment
41 879		2ν <sub>9</sub> +1ν <sub>8</sub>
42 056	4ν <sub>9</sub>	
42 542	5ν <sub>9</sub>	
43 046		
43 066	6ν <sub>9</sub>	
43 341	3ν <sub>4</sub>	
43 574	7ν <sub>9</sub>	
43 879	1ν <sub>9</sub> +3ν <sub>4</sub>	
44 103	8ν <sub>9</sub>	
44 426	2ν <sub>9</sub> +3ν <sub>4</sub>	
44 566		2ν <sub>5</sub> +2ν <sub>8</sub>
44 635		4ν <sub>9</sub> +3ν <sub>8</sub>
44 740		8ν <sub>9</sub> +1ν <sub>13</sub> ; 1ν <sub>9</sub> +3ν <sub>5</sub>
45 018		3ν <sub>9</sub> +4ν <sub>8</sub> ; 7ν <sub>9</sub> +1ν <sub>5</sub>
45 105		8ν <sub>9</sub> +1ν <sub>13</sub>
45 174		
45 261		
45 557		
45 644		
45 731		
45 835		
46 114		
46 201		
46 409		
46 653		

TABLE IV. CD<sub>3</sub>ND<sub>2</sub> spectrum. Assignments based on a transition origin of 40 030 cm<sup>-1</sup>.

Transition energy (cm <sup>-1</sup> )	Assignment	Tentative assignment
41 969	4ν <sub>9</sub>	
42 153		Hindered rotor feature
42 175		Hindered rotor feature
42 240		Hindered rotor feature
42 614	3ν <sub>9</sub> +1ν <sub>4</sub>	
42 959		6ν <sub>9</sub>
43 092	4ν <sub>9</sub> +1ν <sub>4</sub>	
43 432	7ν <sub>9</sub>	
43 478	3ν <sub>4</sub>	
43 570	5ν <sub>9</sub> +1ν <sub>4</sub>	
43 717		6ν <sub>9</sub> +1ν <sub>8</sub>
43 768	3ν <sub>9</sub> +2ν <sub>4</sub>	
43 870	8ν <sub>9</sub>	
43 915	1ν <sub>9</sub> +3ν <sub>4</sub>	
44 078	6ν <sub>9</sub> +1ν <sub>9</sub>	
44 246	4ν <sub>9</sub> +2ν <sub>4</sub>	
44 413		2ν <sub>9</sub> +3ν <sub>4</sub> ; 9ν <sub>9</sub> ; 3ν <sub>4</sub> +1ν <sub>14</sub>
44 600		4ν <sub>4</sub> ; 7ν <sub>9</sub> +2ν <sub>13</sub> ; 7ν <sub>9</sub> +1ν <sub>4</sub>
44 733		5ν <sub>9</sub> +2ν <sub>4</sub>
44 908		3ν <sub>9</sub> +3ν <sub>4</sub> ; 10ν <sub>9</sub>
45 228		6ν <sub>9</sub> +2ν <sub>4</sub>
45 409		4ν <sub>9</sub> +3ν <sub>4</sub> ; 11ν <sub>9</sub>
45 541		2ν <sub>9</sub> +4ν <sub>4</sub> ; 9ν <sub>9</sub> +1ν <sub>4</sub>
45 723		7ν <sub>9</sub> +2ν <sub>4</sub> ; 5ν <sub>4</sub>
45 835		12ν <sub>9</sub> ; 10ν <sub>9</sub> +1ν <sub>14</sub> ; 4ν <sub>4</sub> +2ν <sub>13</sub>
45 905		5ν <sub>9</sub> +4ν <sub>4</sub>
46 030		3ν <sub>9</sub> +4ν <sub>4</sub>
46 217		1ν <sub>9</sub> +5ν <sub>4</sub>

TABLE V. Hartree–Fock results for methyl amine.

Sym	Description	Energy (a.u.)	Geometry (Å)			
			x	y	z	
A'	Ground state ethanelike	−95.240 587	C	−0.002 672	0.000 094	0.000 000
			N	1.453 356	0.022 822	0.000 000
			H	−0.352 686	−0.538 357	±0.873 742
			H	−0.471 751	0.984 926	0.000 000
			H	1.804 371	0.498 452	±0.806 790
A'	3s Rydberg state CNH <sub>2</sub> planar	−95.081 721	C	−0.065 488	0.004 206	0.000 000
			N	1.369 492	0.265 230	0.000 000
			H	−0.319 883	−0.545 456	±0.892 011
			H	−0.563 639	0.966 128	0.000 000
			H	1.890 853	0.391 690	±0.875 684
A''	Excited valence CNH <sub>2</sub> planar	−94.964 642	C	−0.067 759	0.050 549	0.000 000
			N	1.269 509	0.483 142	0.000 000
			H	−0.288 092	−0.549 737	±0.890 142
			H	−0.710 633	0.925 608	0.000 000
			H	1.983 685	0.284 103	±0.915 273

repeated with a (dzp+3s) augmented basis at the fixed equilibrium optimized geometry and the energy is found to vary only slightly (<0.01 a.u.).

The MCSD *ab initio* calculation generates somewhat surprising results for the first excited 3s A' Rydberg state. The highest energy occupied orbital of this state has a 3s Rydberg character composed of both carbon and nitrogen atom 3s orbitals as expected, with a higher occupation (−0.16 vs 0.72) on the nitrogen atom; however, the lower open shell, which should contain a 2p nitrogen electron, also displays 3s Rydberg character from both the nitrogen (10.37) and carbon (0.186) atoms. This MCSD wave function composition suggests that the excitation from the ground state nitrogen lone pair nonbonding 2p orbital to the A' 3s Rydberg state is essentially a two electron transition.

A second MCSD calculation yields the result that the A'' valence state is actually lower in energy than the first 3s A' Rydberg state discussed above. This A'' state has no significant 3s Rydberg character contributing to either of its partially filled open orbitals. Excitation to the A'' valence state involves the redistribution of only one electron. While the MCSD calculation lowers the energy of all three states calculated, it lowers the energy of the ground state and the A'' valence state more than that of the A' Rydberg state.

The energies and geometries obtained by the MCSD calculations are present in Table VII. The optimized geometries for CH<sub>3</sub>NH<sub>2</sub> in these three states are depicted in Fig. 7.

### 3. CASSCF

The full configuration interaction complete active space calculations again start from the RHF results. A small CAS with four electrons into four orbitals (4×4) also produced an A' 3s Rydberg state in which both open shell orbitals have significant Rydberg character, with similar population on the 3s of both carbon and nitrogen (C:0.1853/N:−0.9845 and C:−0.1876/N:0.99835); this again indicates a two-electron transition.

A large CAS calculation is also performed on the first A' 3s Rydberg excited state with 10 electrons into 10 orbitals

(10×10). This calculation reverses the result of the smaller CAS and restores the expected physical picture in which the higher energy open shell has predominately 3s character, and the other has predominately 2p character. The former orbital has some contribution from the 3s on C (−0.2549) and a large contribution from the 3s on N (13.7841). The lower energy orbital has contributions from 2p<sub>y</sub> N (0.6108), 3p<sub>y</sub> N (0.1779) and about half as much contribution from the 3s C as from the 3s N (0.1889).

The small (4×4) CAS gives a much different result from the large CAS for the 3s Rydberg state. This indicates one of the difficulties in performing excited state calculations. The MCSD lowers the ground state and A'' excited valence state energies, but leaves the 3s Rydberg state close to the RHF energy. The small (4×4) CAS calculation produces a 3s Rydberg state with some of the features of the MCSD calculation. The large (10×10) CAS calculation significantly lowers the 3s Rydberg energy and changes the character of the partially filled orbitals, but leaves the ground state closer to the RHF energy than did the MCSD calculation. The various approaches work better or worse for different states: The calculated transition energy for the MCSD calculations is high by about half of the experimental transition energy, while the CAS calculations lower the ground state energy considerably less than the MCSD calculation. The energy results of these CAS calculations are presented in Table VIII.

### 4. CAS-MP2

Failure of the MCSD and CAS calculations to handle the valence and Rydberg states of methyl amine at the same level of accuracy is a clear example of the kind of trouble encountered in excited state calculations. If the same method is used for disparate states, it may well work better for some states than others and accuracy is lost. If different methods are used for disparate states, all consistency is lost, and the results are impossible to interpret. In either instance transition energies and electron distributions are difficult to predict reliably.

TABLE VI. (a) RHF calculated vibrational energies ( $\text{cm}^{-1}$ ) for the  $3s$   $A'$  Rydberg state of methyl amine. (b) Experimental vibrational energies ( $\text{cm}^{-1}$ ) of Ref. 8 for the ground state of methyl amine.<sup>a</sup> (c) RHF calculated vibrational energies ( $\text{cm}^{-1}$ ) for the ground state of methyl amine.

Vibration Number	Description				
(A)					
Species $A'$		$\text{CH}_3\text{NH}_2$	$\text{CH}_3\text{ND}_2$	$\text{CD}_3\text{NH}_2$	$\text{CD}_3\text{ND}_2$
1	N-H Sym. stretching	2887	2099	2887	2086
2	C-H Asym. stretching (squeezing)	3001	3001	2222	2224
3	C-H Sym. stretching (breathing)	2911	2911	2089	2101
4	$\text{NH}_2$ Scissors deformation	1477	1128	1473	1145
5	$\text{CH}_3$ Asym. deformation ( $C$ ) (pancake)	1436	1438	1030	1051
6	$\text{CH}_3$ Sym. deformation ( $A$ ) (umbrella)	1377	1380	1081	1027
7	$\text{CH}_3$ Wagging	1046	1038	715	838
8	C-N Stretching	934	867	884	810
9	$\text{NH}_2$ Wagging	645	504	610	484
Species $A''$		$\text{CH}_3\text{NH}_2$	$\text{CH}_3\text{ND}_2$	$\text{CD}_3\text{NH}_2$	$\text{CD}_3\text{ND}_2$
10	$\text{NH}_2$ Asym. stretching	2999	2238	3006	2222
11	C-H Asym. stretching	3043	3037	2256	2268
12	$\text{CH}_3$ Deformation (twist)	1430	1428	1027	1029
13	$\text{NH}_2$ twist with concerted H bend	844	673	715	608
14	Concerted H wave	1191	1131	1073	947
(B)					
Species $A'$		$\text{CH}_3\text{NH}_2$	$\text{CH}_3\text{ND}_2$	$\text{CD}_3\text{NH}_2$	$\text{CD}_3\text{ND}_2$
1	N-H Sym. stretching	3361	2479	3361	2477
2	C-H Asym. stretching ( $C$ )	2961	2961	2203	2202
3	C-H Sym. stretching ( $A$ )	2820	2817	2077	2073
4	$\text{NH}_2$ Deformation	1623	1234	1624	1227
5	$\text{CH}_3$ Asym. deformation ( $C$ )	1473	1468	1065*	1065*
6	$\text{CH}_3$ Sym. deformation ( $A$ )	1430	1430	1142	1123
7	$\text{CH}_3$ Wagging	1130	1117	913	880
8	C-N Stretching	1044	997	973	942
9	$\text{NH}_2$ Wagging	780	624	740	601
Species $A''$		$\text{CH}_3\text{NH}_2$	$\text{CH}_3\text{ND}_2$	$\text{CD}_3\text{NH}_2$	$\text{CD}_3\text{ND}_2$
10	$\text{NH}_2$ Asym. stretching	3427	2556	3427	2556
11	C-H Asym. stretching	2985	2985	2236	2238
12	$\text{CH}_3$ Deformation	1485*	1485*	1077	1077
13	$\text{NH}_2$ twist	1455*	1140*	1416	1110*
14	$\text{CH}_3$ Wagging	1195*	1187	910*	910
(C)					
Species $A'$		$\text{CH}_3\text{NH}_2$	$\text{CH}_3\text{ND}_2$	$\text{CD}_3\text{NH}_2$	$\text{CD}_3\text{ND}_2$
1	N-H Sym. stretching	3391	2453	3391	2453
2	C-H Asym. stretching ( $C$ )	2919	2919	2157	2157
3	C-H Sym. stretching ( $A$ )	2843	2843	2051	2050
4	$\text{NH}_2$ Deformation	1625	1221	1622	1223
5	$\text{CH}_3$ Asym. deformation ( $C$ )	1461	1461	1052	1051
6	$\text{CH}_3$ Sym. deformation ( $A$ )	1428	1429	1148	1122
7	$\text{CH}_3$ Wagging	1142	1122	942	901
8	C-N Stretching	1035	990	959	917
9	$\text{NH}_2$ Wagging	824	641	754	612
Species $A''$		$\text{CH}_3\text{NH}_2$	$\text{CH}_3\text{ND}_2$	$\text{CD}_3\text{NH}_2$	$\text{CD}_3\text{ND}_2$
10	$\text{NH}_2$ Asym. Stretching	3473	2561	3472	2561
11	C-H Asym. Stretching	2952	2952	2191	2191
12	$\text{CH}_3$ Deformation	1476	1474	1064	1026
13	$\text{NH}_2$ twist	1311	762	1233	1068
14	$\text{CH}_3$ Wagging	937	1195	765	672

<sup>a</sup>Bands not directly observed.

A new method has been introduced by Roos<sup>32,33</sup> and Davidson<sup>34,35</sup> which may well revolutionize excited state calculations. This CAS SCF many-body perturbation theory scheme (CAS MP2) succeeds in lowering the energy of each state and predicting a transition energy which is in good agreement with the experimental results. The HONDO 8.5 program suite incorporates the Davidson routine. Although a

small ( $4 \times 4$ ) CAS is the starting point for CAS MP2, the resulting open shell orbitals are more consistent with our expectations: a  $3s$  Rydberg ( $-0.1809$  C/ $1.1728$  N) excited orbital and a  $2p_y/3p_y$  N orbital with no significant  $3s$  contributions from either C or N atomic orbitals. The energy results for the CAS MP2 calculations are summarized in Table IX.

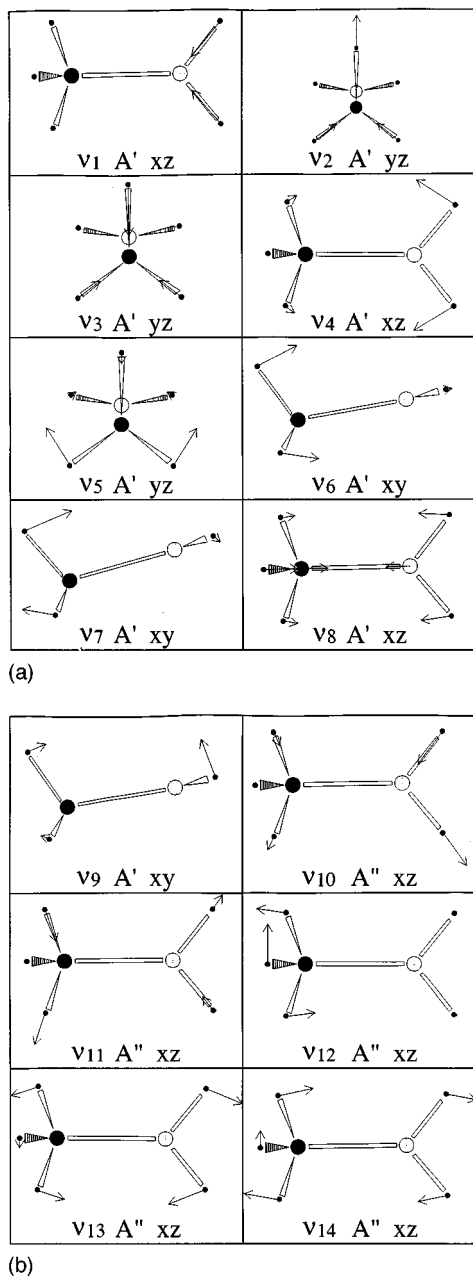


FIG. 6. Excited state vibrations from the RHF calculation. The numbering follows the ground state assignments of Ref. 8. The symmetry of the vibration is indicated. The nuclear positions and motions have been projected into the  $xy$ ,  $yz$ , or  $xz$  planes, and this projection plane is also indicated in the figure. Refer to Fig. 7(D) for the coordinate system axes used.

#### IV. DISCUSSION

In this section we discuss first the assignment details of the observed spectra and then suggest options for the nature of the transition itself based on the experiments and *ab initio* calculations.

##### A. Origin and vibrational assignments

The assignment of vibrations for an excited state which has a large geometry change relative to the ground state equilibrium geometry can often be a daunting task. One has no reason to believe that the transition origin is observed in the spectrum in such an instance. Previous studies, nonetheless,

suggest that the origin of the first electronic transition of methyl amine is one of the observed features in the spectrum.

One clear pattern that emerges from the lower energy region of the spectrum of all the isotopes of methyl amine studied is of a somewhat irregular progression. This recurring set of differences (see Tables I through IV) is consistent with previously reported observations. The peak spacings can be readily associated with the RHF predictions for the amine wagging mode  $\nu_9$  at  $645\text{ cm}^{-1}$  for  $\text{CH}_3\text{NH}_2$  (see Table VI). The RHF calculated vibration (for either the  $A'$  or the  $A''$  excited state) appears to be in good agreement with the spacing between several of the observed peaks. This coincidence of calculated and observed vibrational energies is the key to making appropriate, believable assignments for the observed transitions.

The first four features of the  $\text{CH}_3\text{NH}_2$  spectrum (Figs. 1 and 2) can be assigned employing only two of the theoretically predicted vibrational modes in the excited state. The  $n=3, 4, 5$  overtones of the  $645\text{ cm}^{-1}$   $\nu_9$  "amine wagging" mode and  $n=3$  of the  $1191\text{ cm}^{-1}$   $\nu_{14}$  "concerted H wave" mode can be assigned to the observed features. This would lead to a  $0_0^0$  transition energy of  $39\,753\text{ cm}^{-1}$  ( $=41\,688\text{ cm}^{-1} - 3 \times 645\text{ cm}^{-1}$ ) for  $\text{CH}_3\text{NH}_2$ ; however, this simple approach to unraveling the methyl amine spectrum cannot be sustained when applied to the spectra of the other isotopes. We thus reject it as a viable approach.

A more internally consistent picture for assignment of the transition origins and excited state vibrational energies of all the studied isotopic methyl amine species arises if one employs both the calculated zero point energies to predict the isotopic origin blue shifts from the  $0_0^0$  of  $\text{CH}_3\text{NH}_2$  as well as the vibrational energies themselves. The ground state experimental vibrational mode energies of Lord and Grey can be used in this evaluation. The difference between the ground and excited state zero point energies for each isotope gives an estimate of the shift in transition energy for each deuterated isotope from the protonated parent  $\text{CH}_3\text{NH}_2$ . This scheme leads to expected  $0_0^0$  transition shifts for each deuterated isotopomer of  $\text{CH}_3\text{NH}_2$  from the  $\text{CH}_3\text{NH}_2$   $0_0^0$ . The shift results, based on the experimental ground state zero point energy (see Table VI), are ca.  $+200\text{ cm}^{-1}$  for  $\text{CH}_3\text{ND}_2$  and  $\text{CD}_3\text{ND}_2$  and ca.  $0\text{ cm}^{-1}$  for  $\text{CD}_3\text{NH}_2$ . Similar shifts are obtained using the RHF ground state numbers (see Table VI).

Employing both the zero point energy isotopic shifts calculated above and any single vibration of the excited state will still not generate a self-consistent picture of the vibronic structure and origin. A complete and self-consistent analysis for both the vibronic structure and origins of the set of methyl amine isotopic spectra can be achieved, however, if the two amine vibrations "amine scissors" ( $\nu_4$ ) and amine wagging ( $\nu_9$ ), are employed. These modes have a calculated excited state  $3s$   $A'$  energy of  $1477$  and  $645\text{ cm}^{-1}$ , respectively (see Table VI). The previously assigned  $n=3$  concerted H wave  $\nu_{14}$  ( $1191\text{ cm}^{-1}$ ) feature would then be reassigned as  $2\nu_4 + \nu_9$  ( $=3599\text{ cm}^{-1}$ ) for  $\text{CH}_3\text{NH}_2$ .

Using the anticipated isotope shifts for the various deuterated species and the  $\nu_4$  and  $\nu_9$  modes, nearly all the major features in the low energy region of the spectra of all the studied isotopes can be assigned. The origins of the  $3s$   $A'$

TABLE VII. Multiconfiguration singles and doubles (MCSD) calculation results for methyl amine.

Sym	Description	Energy (a.u.)	Geometry (Å)			
			x	y	z	
A'	Ground state ethanelike	-95.520 361 231	C	-0.011 591 918 5	-0.001 245 245 7	0.000 000 000 0
			N	1.468 562 479 8	0.016 731 011 9	0.000 000 000 0
			H	-0.355 933 751 5	-0.539 574 420 5	±0.875 267 960 8
			H	-0.474 454 794 9	0.986 680 798 4	0.000 000 000 0
			H	1.805 827 402 5	0.502 507 353 1	±0.807 609 603 5
A'	3s Rydberg state CNH <sub>2</sub> planar	-95.190 541 585	C	-0.048 727 982 3	-0.016 567 420 9	0.000 000 000 0
			N	1.376 856 178 5	0.223 003 688 9	0.000 000 000 0
			H	-0.338 136 797 7	-0.551 000 622 3	±0.891 575 579 7
			H	-0.520 049 418 7	0.980 134 786 4	0.000 000 000 0
			H	1.875 249 472 2	0.421 731 045 4	±0.868 908 411 4
A''	Excited valence CNH <sub>2</sub> planar	-95.208 332 436	C	-0.052 917 052 1	0.010 510 727 8	0.000 000 000 0
			N	1.294 785 880 0	0.311 006 730 4	0.000 000 000 0
			H	-0.364 277 295 1	-0.558 084 859 3	±0.907 706 400 6
			H	-0.628 544 527 8	0.951 626 876 8	0.000 000 000 0
			H	1.998 767 208 3	0.385 528 642 1	±0.945 704 534 1

Rydberg state transition for the various isotopic species are thus: CH<sub>3</sub>NH<sub>2</sub>—39 770 cm<sup>-1</sup>; CD<sub>3</sub>NH<sub>2</sub>—39 703 cm<sup>-1</sup>; CH<sub>3</sub>ND<sub>2</sub>—39 985 cm<sup>-1</sup>; and CD<sub>3</sub>ND<sub>2</sub>—40 030 cm<sup>-1</sup>. Note that these experimental isotope shifts are parallel to those calculated and thus expected based on the RHF zero point energies of the first excited state and the ground state zero point energies of Lord and Grey. The included vibrations  $\nu_4$  and  $\nu_9$  for the vibronic structure of this transition are physically reasonable since they bring about the structure change from an ethanelike ground state to a planar excited state. The fact that the origins are not directly observed in these spectra but are “predicted” about 1000 cm<sup>-1</sup> below the first ob-

served features is also consistent with a Franck–Condon displaced spectrum due to the large change in equilibrium geometry for the two states involved in the transition.

The presented assignments seem quite reasonable because the RHF vibrational calculations agree well with the observations with regard to both the chosen vibrational modes in the vibronic assignments as well as the total zero point energy transition shifts. Since the calculations of modes and zero point energy are nearly the same for both the 3s A' Rydberg state and the A'' valence excited states, this agreement does not resolve the question of the character of the first observed excited state. We will discuss this point further in the next section. The main strength of these assignments of vibronic structure and origins is that, based on the RHF calculations of ground and excited state vibrations, the isotopic shifts and individual mode assignments are largely independent of the description of the excited electronic state accessed.

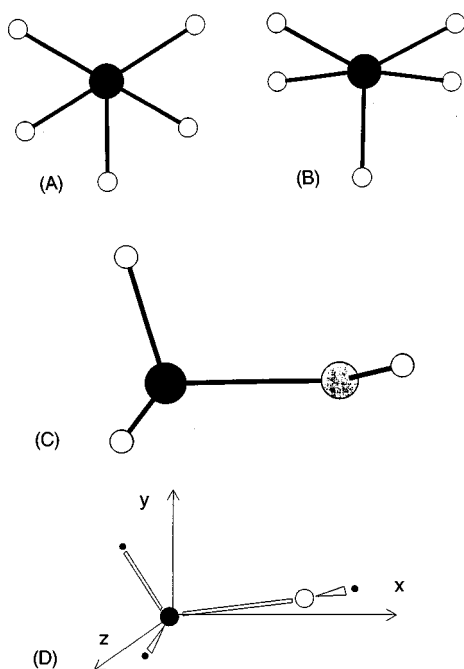


FIG. 7. (A) Ground state geometry of methyl amine (from MCSD calculation). (B) 3s A' Rydberg state geometry of methyl amine (from MCSD calculation). (C) Another view of the 3s Rydberg state geometry of methyl amine (from MCSD calculation). (D) Hartree-Fock geometry of the 3s Rydberg state with axes used for vibrational projections in Fig. 6.

## B. Excited electronic state nature and assignment

The traditional view of low energy Rydberg states is that they are generated by a one electron excitation and that they are often centered predominantly on a single atom (O, N, etc.) in the molecule. The methyl amine and other alkyl amines (ABCO, DABCO) we have studied appear to present a different picture of these excited states. The lowest 3s Rydberg state wavefunction has significant contributions from more than one heavy atom and can often arise from a two electron excitation. This view of the low energy Rydberg states would lead to the mixing of Rydberg states and valence states in which the Rydberg state electron(s) should be thought of as delocalized between the atoms that make up the core. This is actually closer to Mulliken's picture of Rydberg states<sup>2</sup> than the simplified “traditional” view. The Rydberg electron is thus only excluded from a relatively small region associated with the quantum defect. In this picture, even though the energy effects of the quantum defect can be simply parametrized, the structure of the excluded region in

TABLE VIII. CAS Calculation results for methyl amine. See the text for the explanation of the notation.

Symmetry	Description	Size of CAS	Energy (a.u.)	Geometry
$A'$	Ground state	(4×4) dzp	−95.238 047 1	Ethanelike
		(4×4) dzp+3s	−95.238 198 6	
		(10×10) dzp	−95.345 437 9	
$A'$	3s Rydberg	(4×4)	−95.071 715 8	$\text{CNH}_2$ planar
		(10×10)	−95.158 407 7	
$A''$	Valence	(4×4)	−94.938 953 5	$\text{CNH}_2$ planar
		(10×10)	−95.047 958 3	

the core matters and the low-lying Rydberg state participates fully in the dynamics and chemistry of the molecule.

The experimental results do not speak to the problem of electronic state assignment. The high level configuration interaction calculations are motivated by an effort to reconcile experiment and theory. The MCSD calculation opens the possibility that the first excited state of methyl amine is actually an  $A''$  valence state. The contention is supported by a small (4×4) CAS calculation and contradicted by a large (10×10) CAS calculation.

The CAS MP2 calculations do predict a transition energy which is close to the experimental value. Even though we are unable to perform a large CAS MP2 calculation using HONDO 8.5, a (4×4) CAS MP2 calculation seems adequate to describe both the ground and excited states of methyl amine. This result indicates that the first excited states of methyl amine is the 3s  $A'$  Rydberg state, but the  $A''$  valence state cannot be rejected based on this series of calculations. We believe this series of calculations is the most reasonable and accept that the first excited state is a 3s  $A'$  Rydberg state.

### C. High energy region of the spectra and additional electronically excited states

The high energy region of the methyl amine spectrum, unlike the low energy region, is not so readily understood. One can approach an assignment in two ways. First, one can explain the high energy vibronic spectrum of methyl amine by assuming that, like the ground state, the excited state exhibits strong coupling between vibrations: that is, the overtone and combination modes are quite anharmonic. Thus, one expects that the harmonic fit to the observed features becomes worse at higher energies and that the coincidences (Fermi resonance) between features like  $(2\nu_4 + \nu_9)$  and  $3\nu_{14}$  increase. While this approach “works” at a certain level, it does not explain the qualitative appearance of the high energy features. The high energy vibronic features of these spectra of the isotopic methyl amines do indeed appear to be

associated with different progressions and dynamics from those of the low energy region. See Figs. 2 through 5.

An alternative, second point of view, for the assignment of the high energy methyl amine spectrum centers around the suggestion (from theory) that more than one electronic state (at least three, in fact) should be found in the 40 000 to 45 000  $\text{cm}^{-1}$  region. The distribution of peak intensities and the observation that the amine wagging  $\nu_9$  mode progression appears to lose intensity in the middle of the spectrum and then to regain it abruptly for the last 2000  $\text{cm}^{-1}$  of features, also suggests this option. The last several features in the  $\text{CH}_3\text{NH}_2$  spectrum are separated by 670  $\text{cm}^{-1}$  and the last several features in the  $\text{CD}_3\text{ND}_2$  spectrum are separated by 535  $\text{cm}^{-1}$ .

The results of the high level calculations raise additional issues and demand that the presence of a second excited state be seriously considered. The MCSD calculation suggests not only that an  $A''$  valence excitation lies in this region but that it is lower in energy than the two electron excitation to the 3s  $A'$  lowest energy Rydberg state. Thus these calculations challenge the traditional picture of methyl amine energy level structure. The two-electron excitation is a forbidden transition which further suggests that the observed transition could be to the valence state. Additionally, this would explain the appearance of the spectrum in that the two states could couple and present a very complex vibronic structure. If the MCSD result is correct, the lower energy portion of the spectrum is due to the valence  $A''$  excitation. On the other hand, the extent of the possible vibronic interaction for these two similar excitations may well preclude a simple single electronic state description: a pseudo-Jahn–Teller-like coupling between these two states is to be expected.

The large CAS and CAS MP2 calculations indicate that the first excited state of methyl amine is a 3s  $A'$  Rydberg state. If this result is correct, a second 3s Rydberg state which appears in the RHF calculation is also expected in this

TABLE IX. CAS-MP2 Calculation results for methyl amine.

Symmetry	Description	Basis	Energy (a.u.)	Geometry
$A'$	Ground state	dzp	−95.565 985 3	Ethanelike
		dzp+3s	−95.571 689 5	
$A'$	3s Rydberg	dzp+3s	−95.379 733 5	$\text{CNH}_2$ planar
$A''$	Valence	dzp+3s	−95.281 669 1	$\text{CNH}_2$ planar

TABLE X. Vibrational frequencies experimentally observed in the excited state spectrum and calculated for the 3s  $A'$  Rydberg state of methyl amine.

Molecule	$\nu_9$ Observed ( $\text{cm}^{-1}$ )	$\nu_9$ Theory ( $\text{cm}^{-1}$ )	$\nu_4$ Observed ( $\text{cm}^{-1}$ )	$\nu_4$ Theory ( $\text{cm}^{-1}$ )
$\text{CH}_3\text{NH}_2$	642	645	1476	1477
$\text{CD}_3\text{NH}_2$	589	610	1478	1473
$\text{CH}_3\text{ND}_2$	512	504	1128	1128
$\text{CD}_3\text{ND}_2$	486	485	1144	1145

region. If two or three electronic states appear in this region (40 000 to 45 000  $\text{cm}^{-1}$ ) and can all vibronically couple to one another, the assignment of the vibronic details at high energy would indeed be difficult. This is especially true if the geometry of the second Rydberg state is different from the ground state and the first  $3s$  Rydberg state.

Under the present interpretation, the spectrum seems to be dominated by the two amine modes ( $\nu_4$  and  $\nu_9$ ) which bring the ground and excited state geometries in to registry. We may thus not observe the modes that strongly couple the two nearly degenerate excited Rydberg and valence states.

Recent photodissociation studies of methyl amine support the calculations presented here.<sup>31</sup> The hydrogen elimination observed in this study is consistent with the second  $3s$   $A'$  Rydberg state predicted by our RHF calculations which evidences a distortion toward an  $sp^2$  carbon geometry. This state has a large contribution from the  $3s$  orbital on the carbon atom. Such a correspondence between the calculated state and the observed methyl amine photodissociation is particularly interesting with regard to the role of Rydberg states in photochemistry and chemistry of highly excited states.

The main points of this section are that one can have high confidence in the assignment of the vibronic structure for the low energy portion of the methyl amine spectrum and that high the energy portion of the spectrum may well be dominated by a new electronic transition. The vibrational assignments are presented as either firm or tentative in Tables I through IV and in Figs. 2 through 5. A comparison of the experimentally observed excited state vibrations and the RHF prediction is given in Table X.

## V. CONCLUSIONS

Mass resolved excitation spectroscopy and supercooling are employed in this study to obtain data on the electronic transitions in the region 40 000 to 45 000  $\text{cm}^{-1}$  for methyl amine and three of its deuterated analogs:  $\text{CH}_3\text{ND}_2$ ,  $\text{CD}_3\text{NH}_2$ , and  $\text{CD}_3\text{ND}_2$ . Calculations at the RHF, MCSD, and CASSCFMBPT (CAS MP2) levels are used to support and analyze the experimental data. These calculations suggest the following: (1) the lowest excited state is most likely a  $3s$   $A'$  Rydberg state; (2) this state is partially delocalized over the C and N atoms; (3) a valence state of  $A''$  symmetry is also predicted in this region and is, in fact, lower in energy at the MCSD level of theory than the  $3s$   $A'$  Rydberg state; (4) a second  $3s$   $A'$  Rydberg state is found above the other two states, the geometry of which suggests dissociation by hydrogen elimination; and (5) both the lower  $3s$   $A'$  Rydberg state and the  $A''$  valence state are planar for the C– $\text{NH}_2$  moiety of methyl amine.

The experiments are consistent with this two-state picture in the 40 000 to 45 000  $\text{cm}^{-1}$  region. Transition origins and various vibrational modes are identified for the isotopic species. The spectra of all species are dominated by the amine scissors  $\nu_9$  mode and the amine wagging  $\nu_4$  mode. The methyl amine results presented here are quite consistent with the recent studies of ABCO and DABCO low energy Rydberg states.

The improved understanding of methyl amine excited state behavior that results from these studies opens a number of directions for further research into methyl amine vibronic coupling, photodissociation chemistry, and electron and proton transfer, as well as other bimolecular reactions in clusters.

## ACKNOWLEDGMENTS

This work was supported by a grant from the USARO. We wish to thank Professor A. K. Rappé for his help with and discussion concerning the *ab initio* calculational portion of this study.

- <sup>1</sup>G. Herzberg and R. Kolsch, *Z. f. Electrochem.* **39**, 572 (1933).
- <sup>2</sup>R. S. Mulliken, *J. Chem. Phys.* **3**, 506 (1935).
- <sup>3</sup>Q. Y. Shang, C. F. Dion, and E. R. Bernstein, *J. Chem. Phys.* **101**, 118, (1994); R. Disselkamp, Q. Y. Shang, and E. R. Bernstein, *J. Phys. Chem.* **99**, 7227 (1995).
- <sup>4</sup>Q. Y. Shang, P. O. Moreno, and E. R. Bernstein, *J. Am. Chem. Soc.* **116**, 311 (1994).
- <sup>5</sup>J. M. Allen, M. N. R. Ashfold, R. J. Strickland, and C. M. Western, *Mol. Phys.* **74**, 49 (1991).
- <sup>6</sup>J. H. Glowina, S. J. Riley, S. D. Colson, and G. C. Nieman, *J. Chem. Phys.* **73**, 4296 (1980).
- <sup>7</sup>A. E. Douglas and J. M. Hollas, *Can. J. Phys.* **39**, 479 (1961); A. E. Douglas, *Discuss. Faraday Soc.* **35**, 258 (1963).
- <sup>8</sup>A. P. Gray and R. C. Lord, *J. Chem. Phys.* **26**, 690 (1957).
- <sup>9</sup>R. G. Owens and E. F. Barker, *J. Chem. Phys.* **8**, 229 (1940).
- <sup>10</sup>(a) A. P. Cleaves and E. K. Plyler, *J. Chem. Phys.* **7**, 563 (1939); (b) M. Tsaboi, A. Y. Hirakawa, T. Ino, T. Sasaki, and K. Tamagake, *ibid.* **41**, 2721 (1964); (c) M. Tsaboi, A. Y. Hirakawa, and K. Tamagake, *J. Mol. Spectrosc.* **22**, 272 (1967).
- <sup>11</sup>C. J. Purcell, A. J. Barnes, S. Suzuki, D. F. Ball, and W. J. Orville-Thomas, *Chem. Phys.* **12**, 77 (1976).
- <sup>12</sup>D. R. Lide, Jr., *J. Chem. Phys.* **20**, 1812 (1952); **21**, 571 (1953); **22**, 1613 (1954).
- <sup>13</sup>K. Shimoda, T. Nishikawa, and T. Itoh, *J. Phys. Soc. Jpn* **9**, 974 (1954); T. Itoh, *J. Phys. Soc. Jpn* **11**, 256 (1956); K. Shimoda, T. Nishikawa, and T. Itoh, *J. Chem. Phys.* **22**, 1456 (1954).
- <sup>14</sup>L. L. Usyphuk, A. G. Harrison, and J. Wang, *Org. Mass. Spectrosc.* **27**, 777 (1992).
- <sup>15</sup>J. A. Tossell, S. M. Lederman, J. H. Moore, M. A. Coplan, and D. A. Chornay, *J. Am. Chem. Soc.* **106**, 976 (1984).
- <sup>16</sup>J. P. Maier and D. W. Turner, *J. Chem. Soc. Faraday Trans. 2* **68**, 526 (1973).
- <sup>17</sup>N. Ohashi, K. Takagi, J. T. Hougen, W. B. Olson, and W. J. Lafferty, *J. Mol. Spectrosc.* **126**, 443 (1987).
- <sup>18</sup>N. Ohashi and J. T. Hougen, *J. Mol. Spectrosc.* **121**, 474 (1987).
- <sup>19</sup>N. Ohashi, K. Takagi, J. T. Hougen, W. B. Olson, and W. J. Lafferty, *J. Mol. Spectrosc.* **132**, 242 (1988).
- <sup>20</sup>N. Ohashi, K. Takagi, J. T. Hougen, W. B. Olson, and W. J. Lafferty, *J. Mol. Spectrosc.* **137**, 33 (1989).
- <sup>21</sup>M. Oda, N. Ohashi, K. Takagi, and J. T. Hougen, *J. Mol. Spectrosc.* **142**, 57 (1990).
- <sup>22</sup>T. Förster and J. C. Jurgens, *Z. Physik. Chem. B* **36**, 387 (1937).
- <sup>23</sup>E. Tannenbaum, E. M. Coffin, and A. J. Harrison, *J. Chem. Phys.* **21**, 311 (1953).
- <sup>24</sup>M. Tsaboi, A. Y. Hirakawa, and H. Kawashima, *J. Mol. Spectrosc.* **29**, 216 (1969).
- <sup>25</sup>M. Tsaboi and A. Y. Hirakawa, *Can. J. Phys.* **60**, 844 (1982).
- <sup>26</sup>C. J. Maxwell, F. B. C. Machado, and E. R. Davidson, *J. Am. Chem. Soc.* **114**, 6496 (1992).
- <sup>27</sup>E. Kassab, J. T. Gleghorn, and E. M. Evleth, *J. Am. Chem. Soc.* **105**, 1746 (1983).

- <sup>28</sup>J. Syage, R. B. Cohen, and J. Steadman, *J. Chem. Phys.* **97**, 6072 (1992).
- <sup>29</sup>K. Law, M. Schauer, and E. R. Bernstein, *J. Phys. Chem.* **80**, 207 (1984).
- <sup>30</sup>M. Dupuis, F. Johnston, and A. Marquez, *Hondo 8.5 from CHEM-Station* (IBM Corporation, Neighborhood Road, Kingston, 12401, 1994).
- <sup>31</sup>G. C. G. Waschewsky, D. C. Kiechen, P. W. Browning, and L. J. Butler, *J. Phys. Chem.* **99**, 2635 (1995).
- <sup>32</sup>B. O. Roos, P. Linse, P. E. Siegbahn, and M. R. A. Blomberg, *Chem. Phys.* **66**, 197 (1982).
- <sup>33</sup>K. Anderson, P. A. Malmquist, and B. O. Roos, *J. Chem. Phys.* **96**, 1218 (1992); **94**, 5483 (1990).
- <sup>34</sup>C. W. Murray and E. R. Davidson, *Chem. Phys. Lett.* **198**, 451 (1991).
- <sup>35</sup>P. M. Kozlowski and E. R. Davidson, *J. Chem. Phys.* **100**, 3672 (1994).